

Optimization of the design of superconducting inhomogeneous nanowires

This article has been downloaded from IOPscience. Please scroll down to see the full text article.

2008 J. Phys.: Condens. Matter 20 195204

(<http://iopscience.iop.org/0953-8984/20/19/195204>)

View [the table of contents for this issue](#), or go to the [journal homepage](#) for more

Download details:

IP Address: 129.252.86.83

The article was downloaded on 29/05/2010 at 11:59

Please note that [terms and conditions apply](#).

Optimization of the design of superconducting inhomogeneous nanowires

Ilya Grigorenko¹, Jian-Xin Zhu² and Alexander Balatsky¹

¹ Theoretical Division T-11, Center for Nonlinear Studies, Center for Integrated Nanotechnologies, Los Alamos National Laboratory, Los Alamos, NM 87545, USA

² Theoretical Division T-11, Los Alamos National Laboratory, Los Alamos, NM 87545, USA

Received 22 October 2007, in final form 20 March 2008

Published 8 April 2008

Online at stacks.iop.org/JPhysCM/20/195204

Abstract

We study the optimization of the superconducting properties of inhomogeneous nanowires. The main goal of this research is to find an optimized geometry that allows one to maximize the desired property of superconductors, such as the maximum value of the local superconducting gap or total condensation energy. We consider the axially symmetric design of multilayered nanowires with the possibility of adjusting and changing the layer thickness. We use numerical solution of the Bogoliubov–de Gennes equations to obtain the local superconducting gap for different arrangements of inhomogeneous structures. The values of the optimized properties can be up to 300% greater than for a non-optimized geometry. The optimized configuration of multilayers strongly depends on the desired property one wants to optimize and on the number of layers in the nanowire.

(Some figures in this article are in colour only in the electronic version)

1. Introduction

Recent advances in the fabrication and experimental measurement of spatially inhomogeneous superconducting materials open up new opportunities in the optimal design of targeted properties of superconducting materials. Optimal design is an approach in which one calculates the properties of a given structure or device and then optimizes the shape, composition or mutual orientation of the parts of the structure with the purpose of achieving some function or target property of the structure. With a properly chosen geometry (that determines boundary conditions for quantum systems) one can expect enhancement of the target property at certain location, or even observe a ‘quantum mirage’ in confined corral-like nanoscale systems [1].

The ideas of optimal design follow the same line of thinking as in band structure engineering [2, 3] or prediction of a complex materials structure using information-theoretical methods [4]. The notion of optimal design also can be viewed as an extension of similar ideas to the design of decoherence-protected quantum state engineering in quantum computing [5, 6].

In this work we propose to extend the notion of design of quantum states to the case of superconducting materials.

We will focus on superconducting nanostructures. Examples of the specific parameters that one might want to optimize in superconducting materials are the local superconducting gap $\Delta(\mathbf{r})$ and the maximum of the condensate energy $E_{\text{cond}} \propto \int d\mathbf{r} |\Delta(\mathbf{r})|^2$. These are the main target parameters we will focus on below. Specifically, we are going to investigate the interplay between strong spatial inhomogeneities, confinement and geometry effects in superconducting nanoscaled systems. To elucidate this interplay we will focus on the influence of the spatial arrangement of layers of different superconducting materials on the target parameters we mentioned above.

Obviously, the search for optimal design can only be performed using a physically correct and computationally accessible model. In our approach we use the Bogoliubov–de Gennes equation which is well suited to the microscopic description of inhomogeneous superconductors. Since three-dimensional spatial inhomogeneity is not tractable without using a supercomputer, we resort to the case of cylindrical quasi-one-dimensional systems, considering axially symmetric nanowires. Axially symmetric superconducting wires were recently fabricated and have shown their usefulness for prospective measuring devices [7–10].

Before we proceed with the results we will make a few technical comments. Spatial inhomogeneity destroys

translational symmetry and can create localized states on a certain length scale. If the inhomogeneities are created by disorder, they may usually be characterized by simple, low order, and spatially localized correlation functions. However, this approach cannot be applied in the case of engineered, ordered inhomogeneities. In this case inhomogeneities are characterized by spatially delocalized correlation functions of high order. As a result, this problem is not tractable analytically. One needs to use numerical solutions with a fine mesh and at the same time allow for variations in the solution as we search for an optimized configuration. This approach was not possible computationally 10 years ago and has only now become feasible.

In our approach we abandon the usual assumption that the designed inhomogeneity can be treated as a small perturbation. Detailed analysis can demonstrate that the size of the space of accessible solutions grows with the maximum allowed amplitude of the inhomogeneities. Thus, a relatively big inhomogeneity may bring new effects and functionalities, which are not accessible by small perturbations. The assumption of relatively large spatial inhomogeneities places our search for optimal configurations beyond the realm of applicability of the Anderson theorem. The Anderson theorem for non-magnetic alloys and zero external field states that to a first approximation the excitation spectra are the same for the alloy as for the pure metal [11]. This theorem resorts to the assumptions of small spatial inhomogeneity of the pair potential $\Delta(r)$ and chemical similarity of the introduced impurities. Neither of the assumptions hold in configurations that turn out to be optimal.

If designed inhomogeneities are large, a naive strategy to maximize the local superconducting gap $\Delta(\mathbf{r})$ may be achieved by controlling the quasiparticle local density of states at and near the Fermi level. On a deeper level one may expect the interplay between correlations of quasiparticles on the scale of the coherence length ζ and the scale of spatial inhomogeneity. Note that the coherence length may be also modified by the spatial inhomogeneity, thus the problem of the finding the proper length scales should be solved self-consistently.

An important effect that comes into play is the confinement effect [12], when a quasiparticle subband appearing due to finite size quantization happens to be close to the Fermi surface. In this case the density of states is increased, leading to enhancement of the pairing potential.

The pairing potential $\Delta(\mathbf{r})$ may also depend on the finite size of the system via phonon quantization. However, as was shown for thin films [13], this effect is a minor correction to the quasiparticle quantization mechanism mentioned above. Here we leave consideration of the phonon quantization effects for future publications and consider phonons to be the same as in the bulk material.

This paper is organized as follows. In section 2 we present an approach based on numerical solutions of the Bogoliubov–de Gennes equations. In section 3 we discuss the results of numerical solutions and present our main results. In section 4 we discuss the main qualitative finding of the optimal design approach and its applicability to other problems. We conclude in section 5 with a discussion of main results and the outlook for future approaches.

2. Approach and basic facts

In this work we use the Bogoliubov–de Gennes formalism [14]. It is a mean-field formulation of a microscopic theory of weak coupling superconductors, and it is particularly well suited to spatially inhomogeneous problems. It is also appropriate for the relatively small heterostructures in the clean limit that we are interested in.

Using the microscopic theory for inhomogeneous superconductors, one can explore the rich structure in the local density of states (LDOS), which can now be measured directly using STM [15]. Such STM studies, unlike the previous experimental studies [16] which explored only spatially averaged properties, may provide valuable information about local variations of the pair potential $\Delta(\mathbf{r})$.

We are going to use a real space discretization technique [17] that, unlike using a basis of Bessel functions for cylindrically symmetric problems [12, 18], leads to eigenproblem with sparse matrices. In this case the eigenproblem solution can be found much more quickly using sparse iterative solvers. In this work we choose the wire to be hollow to simplify numerical calculations and to avoid uneven real space discretization for the numerical treatment of the singularity near the origin. However, our results will not be changed qualitatively in the case of solid wires of the same size.

The Bogoliubov–de Gennes (BdG) equations for the quasiparticle amplitudes u_n and v_n with excitation energy $E_n > 0$ can be written in a compact form

$$\left(-\frac{\hbar^2}{2m^*}\nabla^2 - \mu\right)\hat{\sigma}_z\hat{\psi}_n(\mathbf{r}) + \Delta(\mathbf{r})\hat{\sigma}_x\hat{\psi}_n(\mathbf{r}) = E_n\hat{\psi}_n(\mathbf{r}), \quad (1)$$

where we denote $\hat{\psi}_n \equiv (u_n, v_n)^T$ and $\hat{\sigma}_x, \hat{\sigma}_z$ are the Pauli matrices. Here μ is the chemical potential. Any effects of the band structure of the material are included in the quasiparticle effective mass m^* . In the presence of a magnetic field one should replace the Laplace operator by $(\mathbf{p} - \frac{e}{c}\mathbf{A})^2$.

The superconducting pair potential $\Delta(\mathbf{r})$ for an s-type superconductor must be determined self-consistently from the solutions of the BdG equations as

$$\Delta(\mathbf{r}) = g(\mathbf{r}) \sum_n u_n(\mathbf{r})v_n^*(\mathbf{r})[1 - 2f(E_n)]\Theta(\hbar\omega_D - E_n), \quad (2)$$

where $f(E_n)$ is the Fermi distribution function, ω_D is the Debye cut-off frequency, $\Theta(\cdot)$ is the step function, and $g(\mathbf{r})$ is the inhomogeneous coupling constant. The summation is performed over the indices n corresponding to $E_n > 0$. Throughout this work, we use the chemical potential $\mu = 0$ and temperature $T = 0$ K. The coupling constant is chosen in order to obtain the bulk value $\Delta_{\text{bulk}} \approx 10$ K. Note that, as in other studies [19], similar model parameters were chosen for illustrative purposes only and were not intended to reproduce realistic materials.

Assuming the z axis to be an axis of the axial symmetry in the wire of length L and imposing periodic boundary conditions along this axis, the solution of equation (1) has the form

$$\hat{\psi}_n(\rho, \phi, z) = \hat{a}_n(\rho) \exp(i\ell\phi) / \sqrt{2\pi} \exp(ik_z z) / \sqrt{L}. \quad (3)$$

The BdG equations for the radial part can be written as

$$\left(-\frac{\hbar^2}{2m^*}\nabla_\rho^2 - \mu\right)\hat{\sigma}_z\hat{a}_n(\rho) + \Delta(\rho)\hat{\sigma}_x\hat{a}_n(\rho) = E_n\hat{a}_n(\rho), \quad (4)$$

where we use the notation

$$\nabla_\rho^2 \equiv \partial^2/\partial\rho^2 + \rho^{-1}\partial/\partial\rho - l^2\rho^{-2} - k_z^2 \quad (5)$$

for the radial part of the Laplace operator. Indices l and $k_z = 2\pi n_z/L$ are the azimuthal quantum number and the wavevector in the z direction, respectively.

To compute the self-consistent solution to both equations (1), (2), we assume an initial guess $\Delta_0(\rho) = \Delta_{\text{bulk}}$ for the order parameter. Then by means of numerical diagonalization, we compute the solutions $u_i(\rho)$, $v_i(\rho)$, for each combination $\{l, k_z\}$, corresponding to $\Delta_0(\rho)$. We use these solutions to generate a new guess for the order parameter.

In order to avoid instabilities during the self-consistent calculations that we found typical for strongly inhomogeneous geometries, we use a simple mixing procedure:

$$\Delta_{\text{mix}}(\rho) = \alpha\Delta_i(\rho) + (1 - \alpha)\Delta_{i-1}(\rho), \quad (6)$$

where α is an adjustable parameter, $0 < \alpha \leq 1$. Initially we set $\alpha = 0.5$. To ensure convergence, we increase the current value of α by 5% if the relative deviation between two subsequent steps $S^i = \max_\rho |\Delta_i(\rho) - \Delta_{i-1}(\rho)| / \max_\rho |\Delta_i(\rho)|$ has decreased, $S^i < S^{i-1}$. And we decrease α by 20% in the opposite case, $S^i > S^{i-1}$.

The computed $\Delta_{\text{mix}}(\rho)$ is used for the next iteration step.

We repeat iterations until we achieve an acceptable level of accuracy ($S^i < 10^{-3}$). After the end of the procedure, we perform an additional step with $\alpha = 1$ to ensure convergence of the obtained solution. It usually takes 50–100 iterations to converge.

3. Results

3.1. Homogeneous wires

In order to check our simulations we first reproduce the bulk limit by considering a relatively big system. We assume a hollow homogeneous cylindrical wire with zero value boundary conditions on the inner and outer surfaces. For such small systems the role of the boundary conditions, as we see later, is crucial. The zero boundary conditions we chose do not imply necessarily contact with a normal metal. It can be vacuum (or just air) outside the wire.

We choose the outer radius of the wire as $R_{\text{max}} = 50$ nm, and the inner radius as $R_{\text{min}} = 0.5$ nm (see figure 1). The length of the wire is set to be $L = 500$ nm with periodic boundary conditions; this is a sufficient approximation for an infinitely long wire. The temperature in all our simulations is set to zero, $T = 0$ K.

We find that the radial part of the self-consistent pairing potential $\Delta(\rho)$ is close to the bulk value with some deviations near the boundaries. The slight rise of the pairing potential can be attributed to the local approximation for the pairing potential in the BdG equations, so it has the nature of the Gibb's

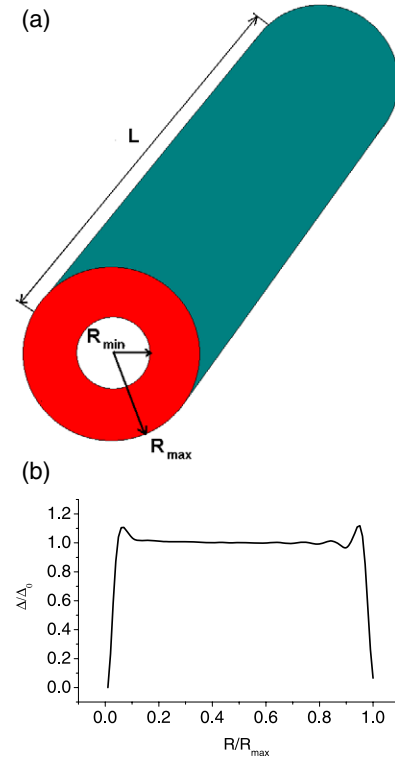


Figure 1. The geometry of the system is depicted in (a) and is represented by an axially symmetric hollow wire. The calculated radial part of the superconducting order parameter $\Delta(\rho)$ (see (b)) is normalized to the bulk value for a uniform infinite hollow superconducting wire with inner radius $R_{\text{min}} = 0.5$ nm and outer radius $R_{\text{max}} = 50$ nm. The length of the wire is chosen to be 500 nm. For our calculations we assume the temperature $T = 0$ K.

phenomenon. Now let us compare a hollow homogeneous cylindrical wire with inner radius R_{min} and outer radius R_{max} , assuming zero boundary conditions, and a homogeneous film of thickness $D = R_{\text{max}} - R_{\text{min}}$. The results of the calculations are shown in figure 2. The spatially dependent superconducting order parameter is normalized to the maximum value Δ_0 for the slab. We chose $R_{\text{max}} = 15$ nm and $R_{\text{min}} = 1.5$ nm. For all our simulations we use a wire length of $L = 500$ nm with periodic boundary conditions. The maximum value of the $\Delta(\rho)$ for the hollow wire is about 30% larger than for a slab. Clearly, for the wire the superconducting order parameter has an asymmetric shape due to different local curvature at different values of ρ . Next we calculate $\Delta(\rho)$ for wires of different thickness. In figure 3 we plot the superconducting order parameter $\Delta(\rho)$ for the fixed outer radius $R_{\text{max}} = 15$ nm and variable inner radius $R_{\text{min}} = 1.5, 3.75, 7.5$ nm. We found that $\max\{\Delta(\rho)\}$ monotonically decreases as a function of R_{min} , together with decreasing of the local curvature.

3.2. Inhomogeneous wires

In this section we focus on a few geometries of inhomogeneous nanowires. In the first geometry we consider a hollow axially symmetric nanowire composed of two layers of two different superconducting materials. We model different materials by using different coupling constants g . We have chosen the

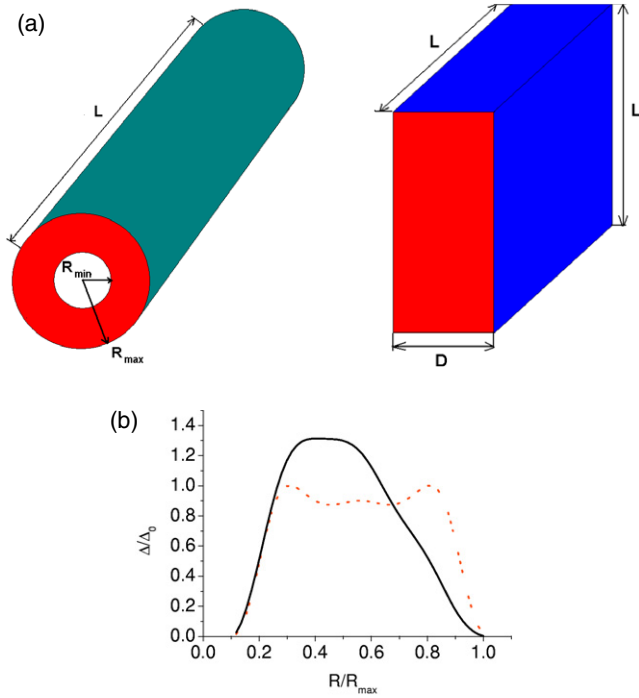


Figure 2. The geometries of the systems under consideration are depicted in (a) and are represented by a hollow wire and a thin film. The calculated radial part of the superconducting order parameter $\Delta(\rho)$ (see (b)) for a uniform hollow superconducting wire with inner radius $R_{\min} = 1.5$ nm and outer radius $R_{\max} = 15$ nm (solid line). The length of the wire is chosen to be 500 nm, and the superconducting order parameter for a uniform superconducting film with the thickness $D = 13.5$ nm (dashed line). The two other dimensions of the film are set to 500 nm. For our calculations we assume the temperature $T = 0$ K.

thicknesses of the layers to be equal, i.e. the first arrangement is $g(\rho) = g_1$, for $R_{\min} < R < (R_{\min} + R_{\max})/2$, and $g(\rho) = g_2$, for $(R_{\min} + R_{\max})/2 < R < R_{\max}$. One can obtain the second arrangement by switching the constants g_1 and g_2 .

Now let us demonstrate an unexpected effect of the geometry on the superconducting order parameter of an inhomogeneous system. We consider a wire which has an inner coaxial layer of a better superconductor with the coupling constant $g_1 = 2g$ and an outer layer with the coupling constant $g_2 = g$. For the second arrangement we consider the inverse layer sequence, namely, the wire has inner coaxial layer of superconductor material with the coupling constant $g_1 = g$ and an outer layer with the coupling constant $g_2 = 2g$. The first choice is depicted in figure 4 by a solid line, and the second choice by a dashed line. Note that the calculated $\Delta(\rho)$ is normalized to the maximum value of Δ_0 for the slab geometry of the same thickness $D = R_{\max} - R_{\min}$. Note that because of the spatial variation of the local curvature the exchange of the superconducting layers leads to non-equivalent results. Interestingly, although for the second arrangement the system has a bigger volume of the better superconductor than in the first arrangement, the maximum value of the pair potential $\Delta(\rho)$ in this case is smaller. This effect is due to local enhancement of the quasiparticles coupling in the effective potential $U_{\text{eff}} \propto \rho^{-2}$ for $\rho \rightarrow 0$, originating from

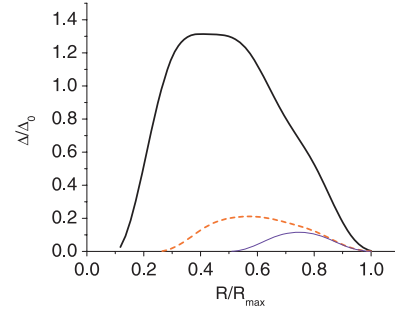


Figure 3. The calculated radial part of the superconducting order parameter $\Delta(\rho)$ for a uniform infinite hollow superconducting wire with the inner radii $R_{\min} = 1.5, 3.75, 7.5$ nm and constant outer radius $R_{\max} = 15$ nm. The length of the wire is chosen to be 500 nm. Note the decrease of the order parameter with decreasing the thickness. For our calculations we assume the temperature $T = 0$ K.

the angular momentum term in the radial part of the Laplacian equation (5).

Now let us consider an inhomogeneous wire composed of three axially symmetric layers. In figure 5 we compared three different arrangements for the three-layer system. We have chosen the layers to be of the same thickness, i.e. $g(\rho) = g_1$ for $R_{\min} < R < (R_{\max} + 2R_{\min})/3$, $g(\rho) = g_2$ for $(R_{\max} + 2R_{\min})/3 < R < (2R_{\max} + R_{\min})/3$ and $g(\rho) = g_3$ for $(2R_{\max} + R_{\min})/3 < R < R_{\max}$. The coupling constant for one of the layers (either g_1 or g_2 or g_3) is set to $2g$, and for the two others it is set to g . For this type of inhomogeneity the best choice that maximizes the superconducting order parameter $\Delta(\rho)$ is the one where the better superconductor is in the middle. Since the layers considered here are thinner than the layers shown in figure 4, the superconducting order parameter of the layer closest to the inner surface is significantly reduced by the proximity effect of the nearest boundary with $\Delta(R_{\min}) = 0$.

Now let us consider an optimal design problem. It is known that the condensation energy E_{cond} is an important quantity that characterizes superconducting systems. Obviously, for an inhomogeneous system it may vary for different arrangements of the superconducting layers. It is interesting to find an optimal configuration that maximizes E_{cond} .

In order to isolate volume effects we assume a superconducting layer of a fixed volume equal to one third of the total volume of the wire: $V_{2g} = \pi(R_{\max}^2 - R_{\min}^2)L/3$. This layer has the coupling constant $2g$. The rest of the material in the wire has the coupling constant g . The problem is to find the best placement of the layer to maximize the condensation energy E_{cond} :

$$E_{\text{cond}} \propto \int_{R_{\min}}^{R_{\max}} \Delta^2(\rho) \rho d\rho. \quad (7)$$

Let the position of the layer's boundary that is closest to the axis of the symmetry be labeled by R , then the layer's boundary closest to the outer surface of the wire will be $R_r = \sqrt{V_{2g}/(\pi L)} + R^2$, where L is the length of the wire.

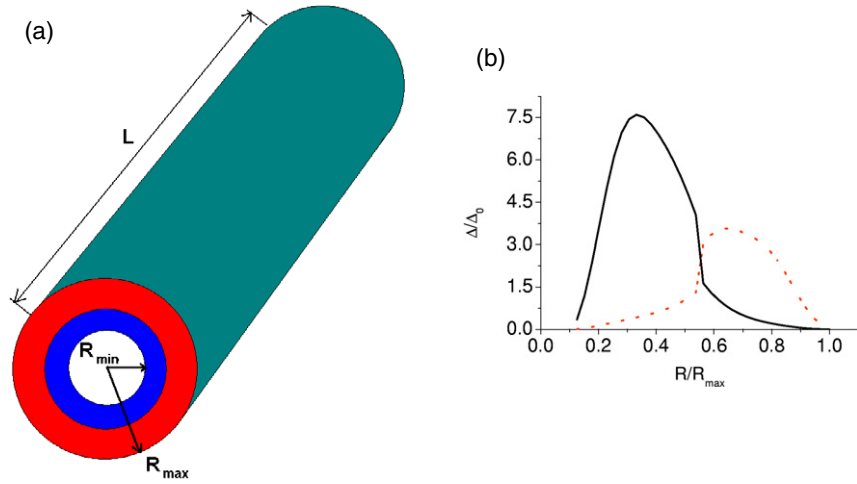


Figure 4. The geometry of the system is depicted in figure 4(a) and consists of two axially symmetric layers. The order parameter $\Delta(\rho)$ (see figure 4(b)) for a non-uniform hollow wire with $R_{\min} = 1.5$ nm and $R_{\max} = 15$ nm. The length of the wire is chosen to be 500 nm. For our calculations we assume the temperature $T = 0$ K. The thick solid line corresponds to the case when the layer with a stronger coupling constant $2g$ closer to the center (dashed line) corresponds to the case when the layer with stronger coupling constant close to the outer surface. The weaker superconductor has the coupling constant g . The thickness of each layer is 6.75 nm. Note the non-equivalence of the arrangements due to the local curvature.

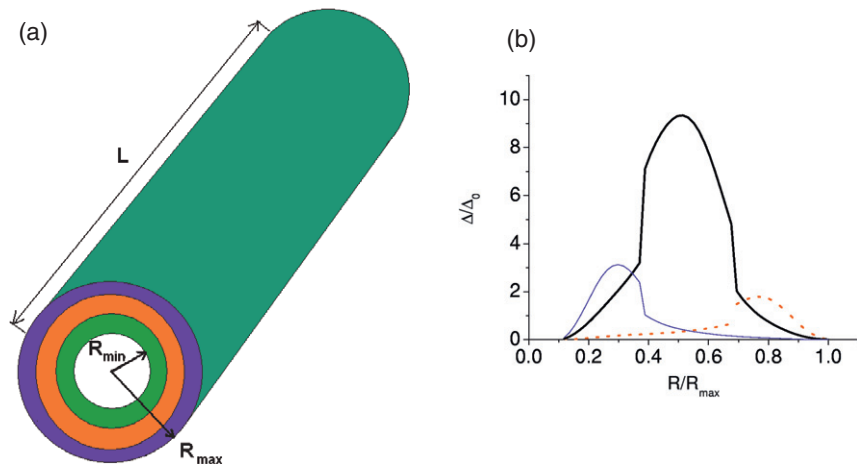


Figure 5. The geometry of the system is depicted in figure 5(a) and consists of three axially symmetric layers. The order parameter $\Delta(\rho)$ (see figure 5(b)) for a non-uniform hollow wire with three layers and three different arrangements—the better superconductor has a doubled coupling constant. $R_{\min} = 1.5$ nm and $R_{\max} = 15$ nm. The length of the wire is chosen to be 500 nm. For our calculations we assume a temperature $T = 0$ K.

In figure 6 we plot the condensation energy E_{cond} normalized to its maximum value E_{max} as a function of its position R . For our simulations we choose $R_{\min} = 1.5$ nm, $R_{\max} = 15$ nm, $L = 500$ nm. One can clearly observe that the condensation energy has a maximum near $R \approx 5$ nm. For this placement the reducing effect from the boundary $\Delta(R_{\min}) = 0$ is minimized, while the effective enhancement of the superconducting order parameter due to the local curvature is still taking place. There are some other local maxima of the condensation energy that we attribute to finite size resonance [12].

As we mentioned above, it is now possible to measure the local density of states (LDOS) directly using a STM technique. In the STM experiment [15] LDOS is proportional to the local differential tunneling conductance. In figure 7 we plot

the calculated local density of states ρ_0 for a homogeneous superconducting nanowire that is determined through

$$\rho_0(\rho, E) = \sum_n [|u_n(\rho)|^2 \delta(E - E_n) + |v_n(\rho)|^2 \delta(E + E_n)]. \quad (8)$$

We again consider a hollow wire with $R_{\min} = 1.5$ nm and $R_{\max} = 15$ nm. The length of the wire is chosen to be 500 nm. We use $E = \Delta_{\text{bulk}}$ for these calculations. In figure 7 one can see relatively big spatial variations of the local density of states due to the confinement of quasiparticles in the cylindrically symmetric boundaries. One may possibly observe these variations by scanning the end face of the wire with a STM tip.

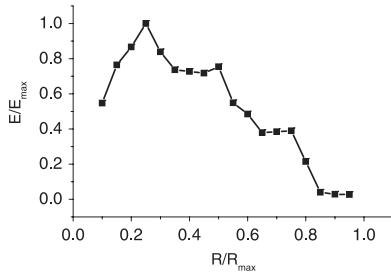


Figure 6. The geometry of the system under consideration is similar to what is shown in figure 5(a). The better superconducting layer is in the middle. The condensation energy $E \propto \int \Delta^2(\rho) \rho d\rho$ of a heterostructure as a function of the position of the better superconducting layer. The better superconductor has a doubled coupling constant $2g$, the worse superconducting layers have g . $R_{\min} = 1.5$ nm and $R_{\max} = 15$ nm. The length of the wire is chosen to be 500 nm. For our calculations we assume a temperature of $T = 0$ K.

4. Discussion

The notion of design of quantum properties is well established. Examples of this quantum state optimization include band structure engineering [2, 3] and engineering of complex material structure [4]. The notion of optimal design also can be viewed as similar to the ideas of decoherence-protected quantum state engineering in quantum computing [5, 6].

We proposed the application of these ideas to superconductors as one example of a macroscopic quantum state. The optimal design approach allows us to investigate the optimal structures that maximize the functional property of nanowires, like maximal condensate energy and superconducting gap.

We find that, depending on the desired property, the specific design is different. Specifically we find that for two-layered superconducting wires the maximal gap is obtained when the superconductor with the stronger pairing potential is placed on the inside. The reason for this enhancement is a confinement effect in the cylindrical geometry.

If one wanted to optimize the maximum critical current one would need to place the stronger superconductor on the outside, because this will be the region where the screening current flows the most. We explicitly demonstrated that, depending on the function one wants to optimize, the superconducting wire design *with the same ingredients* can be very different. On the other hand, in the case of three-layered superconductors we see that the largest gap (with an enhancement factor of about 300%) is obtained when the strongest superconductor is placed in the middle of a sandwich.

The optimal design ideas presented here are applicable to other configurations. One might look at the multilayered structures obtained by molecular beam epitaxy and other methods. Here the combination of superconducting and insulating or magnetic layers (ferromagnetic, multiferroic and other layers) would allow us to investigate the optimal design of multilayered structures with competing interactions. One particularly interesting case is the experiment by Bosovic *et al* [22]. In their multilayered configuration pseudogapped normal regions are alternating with the superconducting regions in

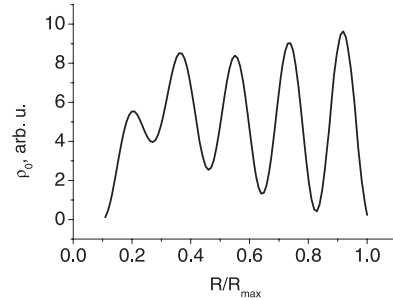


Figure 7. Local density of states (LDOS) $\rho_0(\rho, E)$ for a uniform hollow wire with $R_{\min} = 1.5$ nm and $R_{\max} = 15$ nm, $E = \Delta_{\text{bulk}}$. The length of the wire is chosen to be 500 nm. For our calculations we assume a temperature of $T = 0$ K.

multilayers. The unusual proximity effect has been observed at very large distances of up to 100 Å. We can take these configurations as a guide to how possible future multilayered structures might look. The ideas of optimizing the competing interactions in these configurations are becoming relevant.

5. Conclusion

We consider spatially inhomogeneous superconducting materials with axial symmetry. We also studied the interplay between local curvature and spatial inhomogeneity of the system. We find that due to the cylindrical geometry, different arrangements of superconducting layers are not equivalent because of the different local curvature, and the interchange of the sequence of the layers gives different results. We find that placing the better superconducting material layer closer to the symmetry axis results in a higher values of the pairing potential. However, this is not true in the case when this layer is sufficiently thin. In this case the boundary effects will reduce the effect of the small local curvature. We have proved this for the case of three layers.

We also studied the optimal design problem of placing of the better superconducting layer to achieve the maximum pairing potential. The optimal placement is a result of a compromise between the local curvature effects and effect of the close boundaries. For more complicated geometries and a larger number of layers one should perform the search with the help of global optimization techniques like genetic algorithms. The obtained solutions will most likely not be accessible with any known analytical methods.

For the ultrathin nanostructures we considered in this work, localized impurity effects and phase fluctuations may play a significant role. The impurities and defects can be modeled on the mean-field level by introducing localized impurity potentials, similar to what was done, for example, in [24]. The phase fluctuation effects may compete with the enhancement of the pairing potential due to quantum confinement of quasiparticles in the cylindrical geometry of a nanowire. However, such an effect goes beyond the mean-field BdG theory used in this work. The effect of quantum fluctuations may be an interesting topic to study in the future.

As a possible way to extend our research, we consider the study of non-equilibrium transport properties

of inhomogeneous nanowires (supercurrent distribution, etc). Since the nanowires we consider are much smaller than the characteristic field screening length, the inhomogeneity of the pairing potential will not play a significant role for relatively small fields and currents. However, for larger currents, closer to the critical value, the geometry and size effects may significantly change non-equilibrium characteristics of inhomogeneous superconducting nanowires, resulting in higher values of the critical current. It may also be interesting to study how the value of the critical current depends on the length of the nanowire, and how the pairing potential changes along a nanowire of finite length.

We believe that optimal design has a bright future in nanoscience since it has the potential to convert the available computational power into an improvement of the target properties of rationally structured materials and may substantially increase the efficiency of engineered devices.

Acknowledgment

This work was carried out under the auspices of the National Nuclear Security Administration of the US Department of Energy at Los Alamos National Laboratory under contract no. DE-AC52-06NA25396.

Appendix

We have already outlined in the introduction the main points of our approach. Here we will elaborate on the more technical details of our numerical approach. In our simulations the radial part of the Bogoliubov–de Gennes equations (equation (4)) has a singularity at the origin $\rho = 0$ that needs an uneven discretization mesh and mixed type boundary conditions [12]. In order to avoid these complications, we restricted ourselves to the consideration of hollow cylinders with inner radius R_{\min} and outer radius R_{\max} . We assume Dirichlet type boundary conditions, namely:

$$u_n(R_{\min}) = u_n(R_{\max}) = v_n(R_{\min}) = v_n(R_{\max}) = 0. \quad (\text{A.1})$$

Then we introduce a transformation

$$\hat{a}(\rho) = \hat{b}(\rho)/\sqrt{\rho} \quad (\text{A.2})$$

that removes in equation (4) the term with the first derivative with respect to ρ :

$$\left(-\frac{\hbar^2}{2m^*} \partial^2 / \partial \rho^2 - (l^2 - 1/4) \rho^{-2} - k_z^2 - \mu \right) \hat{\sigma}_z \hat{b}_n(\rho) + \Delta(\rho) \hat{\sigma}_x \hat{b}_n(\rho) = E_n \hat{b}_n(\rho). \quad (\text{A.3})$$

The transformation equation (A.2) guarantees that the discretized Hamiltonian in equation (A.3) is represented by a symmetric matrix that ensures much faster numerical diagonalization.

The radial part of the Bogoliubov–de Gennes equations (A.3) is discretized on a equidistant mesh in real space. For this purpose we use the 13th order 12-point discretization rule for the second derivative [20]. The exact diagonalization of the resulting sparse matrix is then performed numerically using the ARPACK eigensolver [21] available freely on the web [23]. We performed a comparison of the numerical results and the analytical solution available for $\Delta(\rho) \equiv 0$, and find a good agreement using the number of discretization points $N = 200$.

For every iteration step of the self-consistent calculations, the numerical diagonalization procedure is performed for different values of the wavevector k_z and the azimuthal quantum number l . The procedure stops when no eigenvalues lay in the Debye window determined by $\hbar\omega_D$.

References

- [1] Manoharan H C, Lutz C P and Eigler D M 2000 *Nature* **403** 512–5
- [2] Franceschetti A and Zunder A 1999 *Nature* **402** 60
- [3] Dudiy S V and Zunder A 2006 *Phys. Rev. Lett.* **97** 046401
- [4] Ceder G 1998 *Science* **280** 1099
- [5] Yu T and Eberly J H 2002 *Phys. Rev. B* **66** 193306
- [6] Grigorenko I A and Khveshchenko D V 2005 *Phys. Rev. Lett.* **95** 110501
- [7] Young D P, Moldovan M and Adams P W 2004 *Phys. Rev. B* **70** 064508
- [8] Hopkins D S, Pekker D, Goldbart P M and Bezryadin A 2005 *Science* **308** 1762
- [9] Hadfield R H, Miller A J, Nam S W, Kautz R L and Schwall R E 2005 *Appl. Phys. Lett.* **87** 203505
- [10] Doh Y-J, van Dam J A, Roest A L, Bakkers E P A M, Kouwenhoven L P and De Franceschi S 2005 *Science* **309** 272
- [11] Anderson P W 1961 *Proc. 8th Conf. on Low Temperature Physics* (Toronto: University of Toronto Press)
- [12] Shanenko A A and Croitoru M D 2006 *Phys. Rev. B* **73** 012510
- [13] Hwang E H, Das Sarma S and Strosio M A 2000 *Phys. Rev. B* **61** 8659
- [14] de Gennes P G 1966 *Superconductivity of Metals and Alloys* (New York: Benjamin)
- [15] Hudson E W, Lang K M, Madhavan V, Pan S H, Eisaki H, Uchida S and Davis J C 2001 *Nature* **411** 920
- [16] Golubov A A and Hartann U 1994 *Phys. Rev. Lett.* **76** 3602
- [17] Virtanen S M M and Salomaa M M 2001 *Comput. Phys. Commun.* **142** 391
- [18] Maki K and Kato M 2004 *Physica C* **73** 408
- [19] Zhu J-X and Ting C S 1998 *Phys. Rev. B* **57** 3038
- [20] Chelikowsky J R, Chadi D J and Binggeli N 2000 *Phys. Rev. B* **62** R2251
- [21] Sorensen D C 1995 *Invited Paper in SVD and Signal Processing, III* ed M Moonen and B De Moor (Amsterdam: Elsevier)
- [22] Bosovic I *et al* 2003 *Nature* **422** 873
- [23] The ARPACK homepage is located at the address <http://www.caam.rice.edu/software/ARPACK>
- [24] Martin I, Balatsky A V and Zaanen J 2002 *Phys. Rev. Lett.* **88** 097003